

Gas & Galaxy Evolution
*ASP Conference Series, Vol. **VOLUME**, 2000*
J. E. Hibbard, M. P. Rupen and J. H. van Gorkom, eds.

Gas Dynamics in Galaxy Mergers

J. E. Barnes

*Institute for Astronomy, University of Hawaii, 2680 Woodlawn Drive,
Honolulu HI, 96822*

Abstract. In interacting and merging galaxies, gas is subject to direct hydrodynamic effects as well as tidal forces. One consequence of interactions is the rapid inflows of gas which may fuel starbursts and AGN. But gas dynamics is not limited to inflows; a small survey of equal-mass and unequal-mass encounters produces a wide variety of features, including plumes between galaxies, extended disks formed by infall of tidal debris, and counterrotating nuclear disks. An even richer spectrum of behavior awaits better thermodynamic models for gas in merging galaxies.

1. Background

It has long been recognized that interstellar material plays an important role in galaxy interactions. Spitzer & Baade (1951) described fast collisions of galaxies as essentially hydrodynamic affairs. While emphasizing that stellar dynamics governs the outcome of galaxy encounters, Toomre & Toomre (1972) anticipated more than a decade of numerical work in suggesting that interactions ‘bring *deep* into a galaxy a fairly *sudden* supply of fresh fuel’.

The mechanics of this fueling process seem fairly clear. Negroponte & White (1983) found central concentrations of gas in simulated mergers of gas-rich disk galaxies, but the low resolution of their models left the physics uncertain. Noguchi (1987, 1988) and Combes, Dupraz, & Gerin (1990) showed that tidal encounters trigger bar formation in stellar disks and that *gravitational* torques exerted by these bars extract angular momentum from the gas. Hernquist (1989) reported rapid gas inflows in minor mergers where a disk galaxy swallows a small companion; in these experiments the gravitational torques driving the gas inward were generated by both the stellar disk and the companion. Barnes & Hernquist (1991, 1996) modeled major mergers between disk galaxies. This work extended the gravitational inflow picture to show how orbital decay could deliver $\sim 5 \times 10^9 M_\odot$ of gas within the central 100 pc of a merger remnant; such massive gas clouds are common in the central regions of infrared-selected galaxies, many of which are merger remnants (Sanders & Mirabel 1996). Hernquist & Barnes (1991) simulated the formation of a counterrotating gas disk in the aftermath of a major merger. Misaligned or counterrotating disks are found in both merger remnants (Schweizer 1982) and elliptical galaxies (e.g. Bender 1990), strengthening the hypotheses that merging disk galaxies form elliptical galaxies (Toomre & Toomre 1972) and that the centralized starbursts which power lumi-

nous infrared galaxies represent the formation of the cores of elliptical galaxies (e.g. Kormendy & Sanders 1992).

Existing simulations are still incomplete in one key respect: they don't really capture the *thermodynamics* of the gas. Early studies used 'sticky particles' to mimic effects of dissipation. Hernquist and co-workers adopted 'smoothed particle hydrodynamics' (SPH) techniques which can include radiative heating and cooling. But in practice, radiative cooling is usually cut off below 10⁴ K to prevent catastrophic instabilities, and most of the gas remains near this cut-off temperature throughout the simulation. Consequently, simulations including radiative processes are all but indistinguishable from those using an isothermal equation of state (Barnes & Hernquist 1996).

At this point there are two options. One is to adopt the isothermal gas model and survey a range of encounters. The other is to try to develop models which represent the thermodynamics of a multi-phase ISM. Below I discuss both.

2. Isothermal Encounter Survey

Isothermal simulations are relatively cheap, so an encounter survey is possible with modest computers. I chose four encounter geometries, and ran each once with a galactic mass ratio of 1:1 and once with a mass ratio of 3:1. Table 1 lists inclinations i and pericentric arguments ω for the four encounter geometries; in the 3:1 encounters i_1 and ω_1 refer to the more massive galaxy. These experiments used the same bulge/disk/halo galaxy models and close parabolic orbits as Barnes (1998, Ch. 4), but here each disk included a gaseous component amounting to 12.5% of the disk mass. In simulation units with $G = 1$, each galaxy in the 1:1 encounters, and each large galaxy in the 3:1 encounters, has total mass $M_{\text{bulge}} + M_{\text{disk}} + M_{\text{halo}} = \frac{1}{16} + \frac{3}{16} + 1 = 1.25$, half-mass radius $r_{\text{half}} \simeq 0.28$, rotation period $t(r_{\text{half}}) \simeq 1.2$, and binding energy $E = -1.07$; the gas has specific internal energy $u_{\text{int}} = 0.014$. The simulations, each using a total of $N_{\text{gas}} + N_{\text{stars}} + N_{\text{halo}} = 24576 + 29696 + 32768 = 87040$ particles, were run with a new N-body/SPH code featuring adaptive smoothing and time-stepping.

Table 1. Disk angles for survey

Geometry	i_1	ω_1	i_2	ω_2
DIRect	0	0	71	30
RETrograde	180	0	-109	30
POLar	71	90	-109	90
INClined	71	-30	-109	-30

Figure 1 summarizes the evolution of two of these encounters. Here E_r is the energy lost in radiative shocks, while ρ is the gas density. Encounter RET 1:1 (left) is the most dissipative of the eight studied here; radiative losses throughout this calculation amount to $\sim 20\%$ of its initial binding energy. These losses occur in large-scale shocks as the two galaxies plow into each other at $t = 1$, separate, and fall back together. Gas densities increase with each burst of dissipation, and by the end of the simulation some 95% of the gas lies in a barely-resolved disk at the center of the merger remnant. In contrast, encounter POL 3:1 (right) is

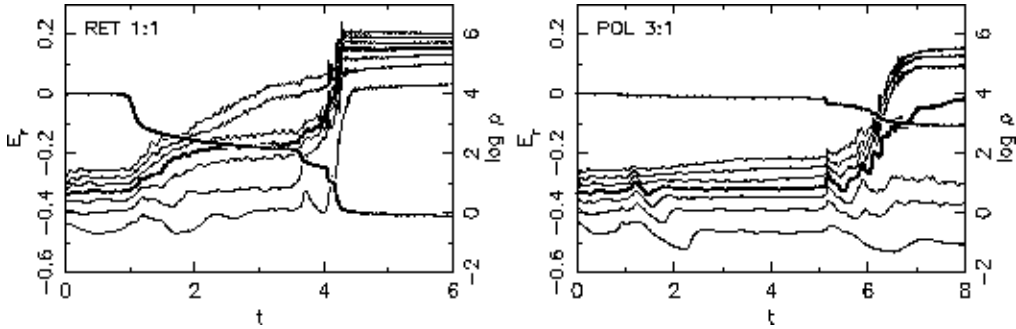


Figure 1. Evolution of two encounters. Single falling curves show E_r , the energy lost to dissipation; rising curves show the first through seventh octiles of the gas density, ρ .

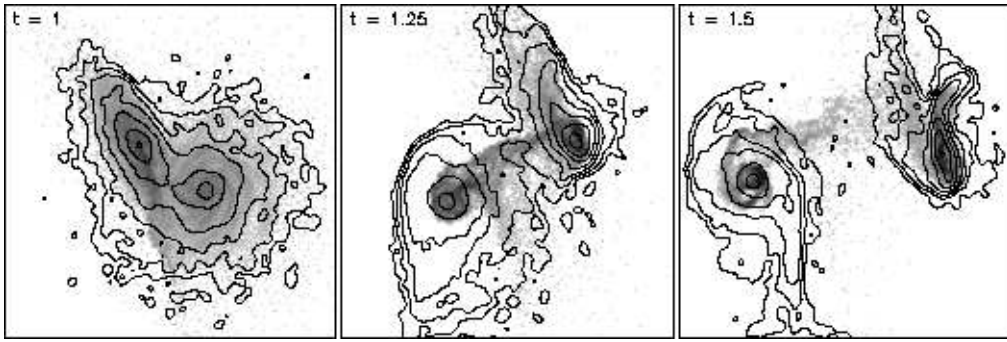


Figure 2. First passage of RET 1:1, viewed face-on to the orbital plane. Contours show stellar surface density in steps of one magnitude; half-tones show gas. Time appears in upper left of each frame. The first two frames are 1.25×1.25 length units; the last frame is 1.5×1.5 length units.

the least dissipative, losing only $\sim 5\%$ of its initial binding energy. The first passage at $t = 1$, while close enough to produce definite tidal features, barely registers in the traces of E_r and ρ . Later passages are more dramatic, eventually driving about 60% into the central regions; most of the remaining gas settles into a warped disk.

The first passage of encounter RET 1:1, shown in Figure 2, exemplifies some consequences of a violent *hydrodynamic* interaction. This encounter's geometry insures that most of the gas suffers strong shocks as the galaxies intersect. By the middle frame shown here, much of the gas in the in-plane disk has been swept into the center. This inflow is driven not by gravitational torques but by hydrodynamic forces; the gas loses its spin angular momentum by colliding with gas in its companion. Gas which escapes being swept inward forms a plume connecting the two galaxies; such structures may be fairly common in interpenetrating encounters (e.g. Condon et al. 1993).

After a tidal encounter, bridges and tails develop from any disk which suffers a reasonably direct passage. While the ends of such features may escape, much of this material is bound to fall back onto its parent – or, if the galaxies have already merged, onto their combined hulks. An example of such re-accretion

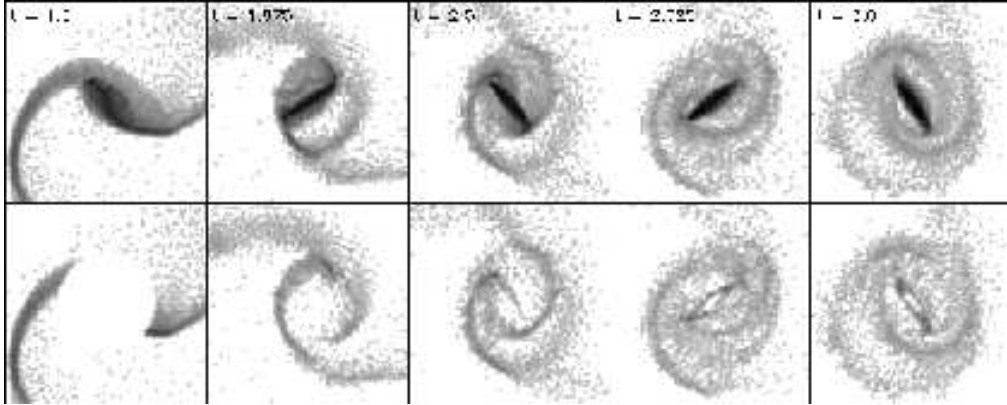


Figure 3. Evolution of large disk in DIR 3:1 after first passage. The upper frames shows all gas; the lower frames show gas re-accreted from tidal features. All frames are 0.8×0.8 length units.

is illustrated in Figure 3. Here the upper row shows gas in the larger disk of encounter DIR 3:1 responding after the direct passage of its lighter companion; note the pronounced bar typically formed in such passages. The lower row shows only the gas which has fallen back from the tidal features. Returning on elongated trajectories, this material is forced onto more circular orbits by shocks, some of which are visible as narrow curvilinear features. By the last frame the re-accreted gas has built up a large disk surrounding the bar.

One consequence of this disk rebuilding is that the gas can be highly sensitive to tidal perturbations on subsequent passages. Stellar disks can't cool down once tidally heated, so they are less responsive and generate broader structures. Figure 4 illustrates the different responses of gas and stars in the second passage of encounter POL 1:1. The first frame shows two fairly relaxed gas disks, each wreathed in stellar debris; at this point the stars and gas have roughly similar distributions. In the second frame the disks have moved past each other, and a pronounced tail extends to the right of the lower galaxy. By the third frame the gas tail extends far beyond the stellar tail, crossing several contours of the stellar distribution; this frame also shows the two galaxies in the process of merging.

In these eight encounters, between 50% and 95% of the gas falls into a compact cloud at the center of each merger remnant. This is consistent with the results of earlier calculations (Negroponte & White 1983; Noguchi 1988; Hernquist 1989; Barnes & Hernquist 1991).

Most of the gas which doesn't wind up in the central cloud nonetheless falls back into the remnant and settles onto closed, non-intersecting orbits. Thus at later times these remnants develop extra-nuclear disks and rings of gas with rather complex morphologies, as shown by the three examples in Figure 5. The remnant of encounter DIR 1:1 contains *two* rings, both rather sparse; the outer one lies within $\sim 10^\circ$ the equatorial plane, while the inner one is tilted by $\sim 70^\circ$. The origin of this tilt is unclear; the tilted ring is largely made up of gas from the $i_2 = 71^\circ$ disk, but it's born in a plane roughly perpendicular to the initial plane of its progenitor. In the remnant of POL 1:1 the extra-nuclear disk contains $\sim 30\%$ of the gas and exhibits an integral-sign warp; this remnant

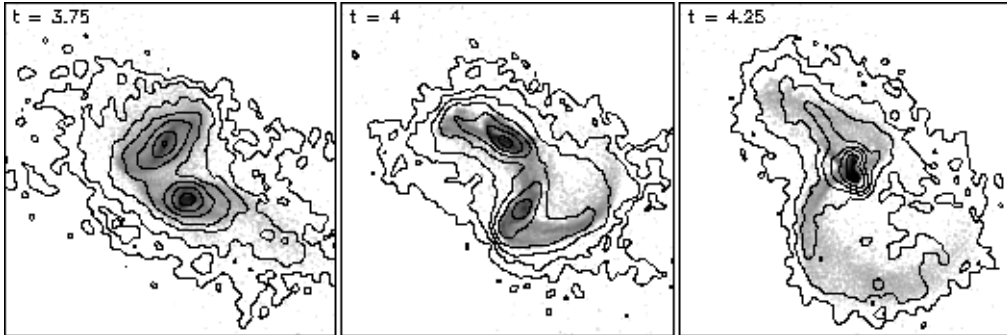


Figure 4. Second passage of POL 1:1. Contours show stellar surface density; half-tones show gas. The first two frames are 1.25×1.25 length units; the last frame is 1.5×1.5 length units.

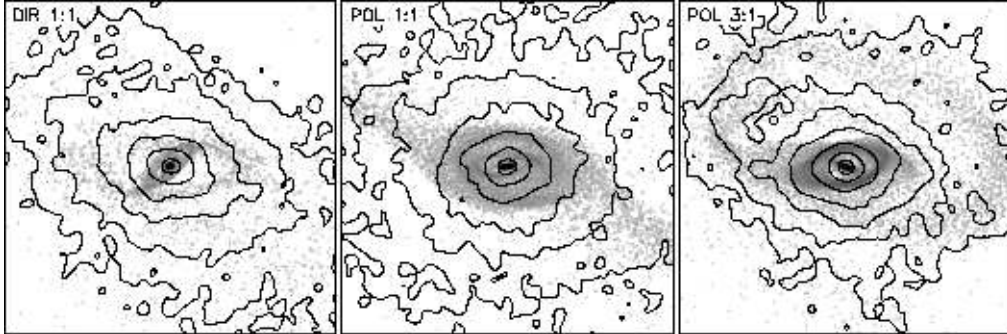


Figure 5. Gas disks in remnants of encounters DIR 1:1 (left), POL 1:1 (middle), and POL 3:1 (right). Contours show stellar surface density; half-tones show gas. All are viewed 30° from edge-on to the stellar distribution. The first two frames are 0.5×0.5 length units; the third frame is 1.0×1.0 length units.

also has a compact nuclear disk, to be discussed below. Finally, the remnant of POL 3:1 has several nested disks and an extended off-center ring composed of material recently accreted from tidal debris. While the outer contour of the stellar distribution roughly parallels the gas ring, the stellar density falls monotonically with distance from the center; unlike the gas, the stars don't form a true ring.

Some of the remnants in this survey have *counterrotating* nuclear disks. The most striking example was produced by encounter POL 1:1; Figure 6 shows that the outer gas disk and the stellar component both rotate in one direction, while the inner gas disk rotates in the other direction. This encounter had the same initial disk angles i_1 , ω_1 , i_2 , and ω_2 as did a previous example of counterrotation (Hernquist & Barnes 1991), but here the first passage was considerably closer. Counterrotation seems insensitive to details of the encounter and simulation code, though the physical mechanism involved is not obvious from a cursory inspection of the simulations. More work is needed to determine the roles of

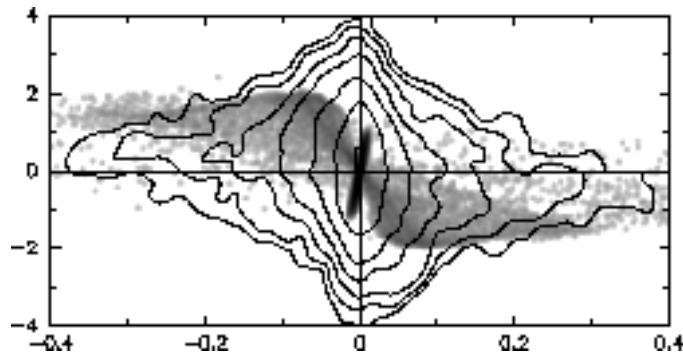


Figure 6. Line-of-sight velocities in remnant POL 1:1, as viewed edge-on to the equatorial plane. Contours show the stellar distribution within a slit along the major axis; half-tone shows *all* gas.

gravitational and hydrodynamic forces in creating counterrotating disks and the *range* of disk angles yielding outcomes like the one in Figure 6.

3. Towards Proper Thermodynamic Models

The forgoing simulations presume that a good part of the ISM behaves somewhat like an isothermal gas at a temperature of 10^4 K. This is probably not a *desperately* bad approximation on scales of order a kpc, but it doesn't address some of the most interesting gas-dynamical effects in merging galaxies – for example, starbursts (Larson & Tinsley 1978), infrared emission (Joseph & Wright 1985), molecular content (Young et al. 1984), and superwinds (Heckman et al. 1996). All but the last of these involve gas which has cooled to well below 10^4 K.

It's hard to model the cold component with any degree of realism; individual GMCs are about 10^{-4} times the total mass of the ISM in a galaxy like ours, and key processes are incompletely understood. One brave attempt by Gerritsen & Icke (1997) allowed gas to cool below 10^4 K, and defined sites of star formation via a simple Jeans criterion; the radiation field of the stars, evaluated in the optically thin limit, was used to heat the gas. This yielded a self-regulating medium with two phases at temperatures of 10^2 K and 10^4 K; as a bonus, the simulations also produced a Schmidt law with index $n \simeq 1.3$. These successes may inhere to almost any approach which balances radiative cooling with heating by star formation.

In infrared-selected galaxies the ISM reprocesses 90% to 99% of the total luminosity (Sanders & Mirabel 1996), and this reprocessing has thermodynamic consequences (e.g. Maloney 1999) missing in optically thin models. Radiative reprocessing could be approximated in SPH by a Monte-Carlo procedure or by solving the diffusion equations, but galactic-scale models will require dramatic improvements in both spatial and temporal resolution; moreover, turbulent, magnetic, and radiation pressure terms may be needed as these probably supplant thermal pressure in a starburst's ISM. This is a tall order for simulators!

If models of cold gas in starbursts are beyond the reach of current simulations then star formation may be included phenomenologically; for example, by

setting $\tau_{\text{sf}} \propto \rho^{-n}$, where τ_{sf} is the star formation timescale, ρ is the local gas density, and $n = 0.5$ for a Schmidt law (Katz 1992; Mihos & Hernquist 1994). This approach seems to reproduce nuclear starbursts, but doesn't readily explain *extended* star formation in systems like NGC 4038/9 (Mirabel et al. 1998) and NGC 3690/IC 694. A more general approach could use the local dissipation rate \dot{u} as a second parameter; for example, setting $\tau_{\text{sf}} \propto \rho^{-n}\dot{u}^{-m}$. This might approximate Jog & Solomon's (1992) model for triggered star formation via compression of molecular clouds.

While cold gas is problematic, it's more straightforward to include hot gas in simulations of galactic collisions. If cooling is simply turned off, gas can be shock-heated to $\sim 10^5$ K in the early stages of an encounter, and finally to the virial temperature of $\sim 10^6$ K in a merger (e.g. Barnes 1998, Ch. 8). But such simulations fail to reproduce the superwinds often seen in starburst galaxies; purely mechanical heating doesn't provide enough energy to drive bulk outflows. Injection of mass and energy by stellar winds, supernovae, or AGN is probably required if the simulations are to resemble real galaxies.

4. Future Directions

While stellar-dynamical modeling of galaxy collisions seems a fairly mature business, the same isn't true of simulations including gas dynamics. Existing codes may do an acceptable job of simulating the behavior of a smooth gas at $\sim 10^4$ K, but the relationship between this hypothetical stuff and the interstellar medium of real galaxies is unclear. I close by listing some possible directions for further work:

- True 3-D modeling of thin disks. In published SPH calculations the smoothing radius exceeds the vertical scale height of the gas. An order of magnitude more gas particles are needed to vertically resolve thin disks.
- Interesting temperature structures. As noted above, attempts to include cold gas face many problems. Hot gas is more easily implemented, but source terms representing stellar processes are probably required to match the observations of this component.
- Self-regulating star formation. Until simulations including cold gas become practical it may be difficult to include "feedback" from star formation. Nonetheless, it may be worth trying simple tricks; e.g., disallowing star formation in recently-shocked gas.
- Magnetic field diagnostics. Polarization maps of continuum emission can provide information on flows in galaxies (e.g. Beck et al. 1999). Simulations including magnetic fields may be able to predict such polarization patterns.

Acknowledgments. Support for this work was provided by NASA grant NAG 5-8393 and by Space Telescope Science Institute grant GO-06430.03-95A.

References

Barnes, J.E. 1998, in Galaxies: Interactions and Induced Star Formation, eds. D. Friedli, L. Martinet, & D. Pfenniger (Springer-Verlag: Berlin), 275

Barnes, J.E. & Hernquist, L.E. 1991, ApJ, 370, L65

Barnes, J.E. & Hernquist, L. 1996, ApJ, 471, 115

Beck, R. et al. 1999, Nature, 397, 324

Bender, R. 1990, in Dynamics and Interactions of Galaxies, ed. R. Wielen (Springer, Berlin), 232

Combes, F., Dupraz, C., & Gerin, M. 1990, in Dynamics and Interactions of Galaxies, ed. R. Wielen (Springer, Berlin), 205

Condon, J.J. et al. 1993, AJ, 105, 1730

Gerritsen, J.P.E. & Icke, V. 1997, A&A, 325, 972

Heckman, T.M. et al. 1996, ApJ, 457, 616

Hernquist, L. 1989, Nature, 340, 687

Hernquist, L. & Barnes J.E. 1991, Nature, 354, 210

Jog, C.J. & Solomon, P.M. 1992, ApJ, 387, 152

Joseph, R.D. & Wright, G.S. 1985, MNRAS, 214, 87

Katz, N. 1992, ApJ, 391, 502

Kormendy, J. & Sanders, D. 1992, ApJ, 390, L53

Larson, R.B. & Tinsley, B.M. 1978, ApJ, 219, 46

Maloney, P.R. 1999, A&AS, 266, 207

Mihos, J.C. & Hernquist, L. 1994, ApJ, 437, 611

Mirabel, I.F. et al. 1998, A&A, 333, L1

Negroponte, J. & White, S.D.M. 1983, MNRAS, 205, 1009

Noguchi, M. 1987, MNRAS, 228, 635

Noguchi, M. 1988, A&A, 203, 259

Sanders, D.B. & Mirabel, I.F. 1996, ARA&A, 34, 749

Schweizer, F. 1982, ApJ, 252, 455

Spitzer, L. & Baade, W. 1951, ApJ, 113, 413

Toomre, A. & Toomre, J. 1972, ApJ, 405, 142

Young, J.S. et al. 1984, ApJ, 287, L65

van der Hulst: How long do the counterrotating disks and warps in the models survive?

Barnes: In DIR 1:1 the tilt of the inner ring decreases with time, while in POL 1:1 the counterrotating nuclear disk seems quite stable. Warps should persist *at least* as long as continued infall from tidal tails feeds in misaligned material.

Dwarakanath: Is there an initial parameter space which does not lead to counterrotating gas disks at the center?

Barnes: Only one of the 1:1 remnants has a *substantial* counter rotating disk. And only one of the 3:1 remnants has a counterrotating disk of any kind. Counterrotation remains the exception rather than the rule.

Mathews: To what extent could the extreme central concentration of gas in post-merger galaxies be due to numerical viscosity?

Barnes: Barnes & Hernquist (1996) varied the artificial viscosity by a factor of three in either direction without changing the resulting central concentration of the gas. Moreover, SPH and sticky particle codes give similar results. It's unlikely that numerical effects play a big role, but proving this beyond a shadow of a doubt is not easy!